16TH EUROPEAN CONFERENCE ON EARTHQUAKE ENGINEERING THESSALONIKI 18 - 21 JUNE 2018

# SEISMIC PERFORMANCE OF A RETAINING WALL SYSTEM CONSIDERING LIQUEFACTION AND SCOUR POTENTIAL

Dimitra Tsiaousi[1], Alfredo Fernandez[2], Jerko Kocijan[3], and Thaleia Travasarou[4]

## ABSTRACT

The seismic performance of a retaining wall system for a water reclamation plant located adjacent to a river in a seismically active area was assessed. In a seismically active area, river banks are likely locations for lateral seismic displacements and lateral spreading, especially when the groundwater level is high and subsurface conditions include liquefiable soils. At this project site, the seismic stability hazard and potential for seismic displacements was further complicated by the potential for significant scouring in the adjacent river along the plant perimeter wall edge.

Advanced two dimensional dynamic numerical analyses using the finite difference software FLAC were conducted to assess the performance of the plant perimeter wall retaining system under seismic loads. The retaining wall system consists of a mechanically stabilized earth (MSE) retaining wall sitting on top of a cement deep soil mixing (CDSM) wall tied back with soil anchors. Wall performance under seismic loads for pre-scour and post-scour conditions of the soil in front of the wall was assessed. The effects of liquefaction were assessed in terms of lateral seismically-induced displacements and seismic earth pressures on the retaining wall system. Sensitivity analyses were also performed to assess the effect of ground water elevation and thickness of the liquefiable layer on the wall performance. Seismic earth pressures resulting from the numerical analyses were compared with conventional simplified methods. These numerical analyses helped to develop seismic performance mitigation alternatives for the retaining wall system.

*Keywords: retaining wall; liquefaction; numerical modeling*

## 1. INTRODUCTION

A water reclamation plant (WRP) which is located in a seismically active area in California and sits on a level plateau about 35 feet above the river channel bottom is undergoing expansion. The site three-dimensional (3-D) topographic model is shown in Figure 1. Grade difference along the river-side of the planned expansion site is accommodated by a mechanically stabilized earth (MSE) retaining wall (about 20 feet exposed height) and sloping ground with inclinations of about 10H:1V (horizontal:vertical). The MSE wall sits on a cement deep soil mixing (CDSM) zone that is approximately 62 feet deep, and was constructed to prevent possible future river scouring to undermine the MSE wall and extent into the WRP area. The CDSM zone is reinforced with steel I-beams along the river side edge of the CDSM wall and the top of the CDSM wall is tied back with pre-tensioned ground anchors (see Figure 2).

The subsurface conditions at the wall location comprise of loose to medium dense sands in the upper 30 feet (below the plateau level), resting on top of dense sands and stiff clays. With the highest

[1] Senior Engineer, Fugro, Walnut Creek, USA, (email: dtsiaousi@fugro.com)
[2] Associate Engineer, Fugro, Walnut Creek, USA, (email: afernandez@fugro.com)
[3] Principal Engineer, Fugro, Commerce, USA, (email: jkocijan@fugro.com)
[4] Principal Engineer, Fugro, Walnut Creek, USA, (email: ttravasarou@fugro.com)

groundwater level possibly as high as about 20 feet below plateau level, the sand layers between about 20- to 30-foot depth are possibly liquefiable.

The topography and subsurface soil conditions leave the WRP site potentially vulnerable to experiencing lateral displacements during earthquakes. Advanced numerical modeling dynamic analyses using the finite differences computer program FLAC (Itasca 2015), were performed to assess the new MSE-CDSM wall performance under seismic conditions. Sensitivity analyses were performed to investigate the effect of soil scour, ground water elevation and thickness of the liquefiable layer on predicted lateral seismically-induced wall displacements. Furthermore, as part of the assessment, seismic earth pressures calculated using FLAC numerical analyses were compared with pressures derived from simplified methods.

The results of the numerical modeling, including the sensitivity analyses, were used to finalize MSE-CDSM wall design and develop better insight into likely wall performance during different earthquake levels. Simplified solutions performed at an earlier design stage to estimate the lateral seismically-induced retaining wall displacements were not considered reliable due to the complexity of the retaining wall system and the subsurface conditions.

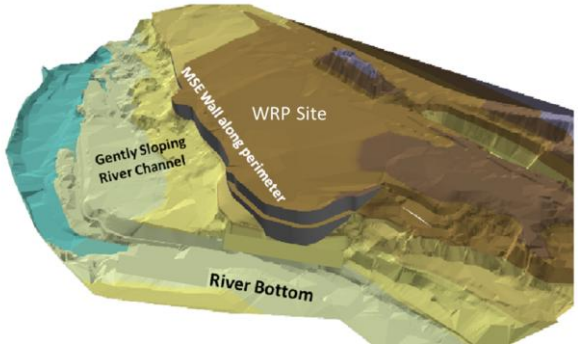


Figure 1. Site 3-D Topographic Model

## 2. ADVANCED NUMERICAL MODELING ANALYSES

Two-dimensional, effective-stress, dynamic analyses were performed using the finite difference computer program FLAC to estimate the liquefied zones and the deformations that occur during strong shaking. FLAC incorporates the ability to model groundwater flow and pore pressure dissipation, and the full coupling between the deformable porous soil skeleton and the viscous fluid flowing within the pore space. FLAC analyses were intended to model the time-dependent, nonlinear behavior associated with liquefaction of sandy loose materials, as well as nonlinear behavior of non-liquefiable clay-type materials that were identified in site characterization.

### *2.1 Idealized Stratigraphy*

The idealized stratigraphy and engineering soil properties beneath the WRP were developed based on boring and CPT data. For the purpose of this study, an idealized cross section (Figure 2), referred to as Base Case, was developed and used in two-dimensional dynamic slope stability analyses. The idealized stratigraphy consisted of loose to medium dense sands in the upper 30 feet (elevation [El.] 1050 to 1020 feet), overlaying a 20-foot thick dense sand layer (El. 1020 to 1000 feet), followed by a 12-foot thick stiff to very stiff clay layer (El. 1000 to 988 feet), and a very dense sand (El. 988 to 950 feet).

The base case analyses included a liquefiable layer from El. 1030 to 1020 feet and ground water table at El. 1030 feet (depth of 20 feet, right between bottom of MSE wall and top of CDSM wall) (Figure 2). Subsequently, several sensitivity analyses were performed to assess the impact of

liquefaction, scour and the effectiveness of potential mitigation measures, as follows:

1) A zone of improved (or replaced) non-liquefiable soil (buffer zone) was introduced between El. 1030 and 1025 feet, extending 30 feet behind the back of the CDSM wall.
2) The post-scour event was analyzed through a series of sensitivity analyses to investigate the impact of reduced passive resistance due to soil removal due to scour (20 feet thick zone down to El. 1010) and soil loosening due to scour and becoming liquefiable (20 feet thick zone between El. 1010 and 990).

### *2.2 Constitutive Models*

Non-liquefiable soils were modeled with the Mohr-Coulomb failure criterion in combination with a nonlinear stress-strain behavior characterized by a three-parameter sigmoidal (Itasca-S3) shaped backbone curve (Itasca 2015). The default Itasca-S3 Hysteresis model computes the nonlinear behavior of the soil by means of a nonlinear stress-strain backbone curve and the associated stress-strain loops that represent the energy dissipated in the soil during seismic loading. The model parameters were fit to approximate target shear modulus reduction curves selected from the available literature for similar soil types, plasticity characteristics, and depth.

The behavior of liquefiable granular foundation soil was modeled using constitutive model UBCSAND (Beaty and Byrne 1998), developed by Professor Peter Byrne and his team at the University of British-Columbia. This model has been extensively calibrated and validated (Giannakou et al. 2011; Giannakou et al. 2012) and has been used recently in the vulnerability assessment of critical structures (Travasarou et al. 2011; Travasarou et al. 2012).

### *2.3 Numerical Model*

The MSE wall was about 20 feet tall (El. 1050 to 1030 ft), and 6 to 17 feet wide. The MSE wall face consisted of concrete blocks 1.5 feet tall and 1 foot wide. Interfaces were modelled between the concrete blocks that allowed relative movement. Strips were also modelled explicitly every 1.5 feet along the MSE wall. The MSE wall was not rigidly connected with the CDSM wall below. The CDSM wall was 62 feet deep (El. of 1030 to 968 ft) and 22 feet wide for the top 30 feet, 8 feet wide for the following 26 feet and 4 feet wide for the bottom 6 feet. A steel I-beam (W36x170) was modelled at the river-side edge of the CDSM wall. Interfaces were modelled along all edges of the CDSM wall. An anchor was connected to the CDSM wall at the top river-side edge. The anchor had an out-of-plane spacing of 7 feet, was 93 feet long (60 feet cable length, 33 feet bonded length) and was installed at an angle of 15 degrees. The anchor was modelled with cable elements and was pre-tensioned at installation.

The model was subjected to one-directional horizontal dynamic loading using time histories. The selected motions were processed to be compatible with a target spectrum developed for "competent-soil" condition with an average shear wave velocity ($V_s$) on the order of 1300 ft/sec. These motions were defined as "outcrop" stiff soil motions and applied at a depth below which the $V_s$ is estimated to be about 1300 ft/sec or greater. A compliant base was used at the bottom of the model (through the use of quiet boundaries in FLAC) to model the half space. Dynamic analyses were performed for three input ground motions consistent with the seismic hazard at the site for return periods of 225 and 475 years, and both polarities were evaluated for each time history. Herein, we are presenting only the results of the most critical polarity of the motions.

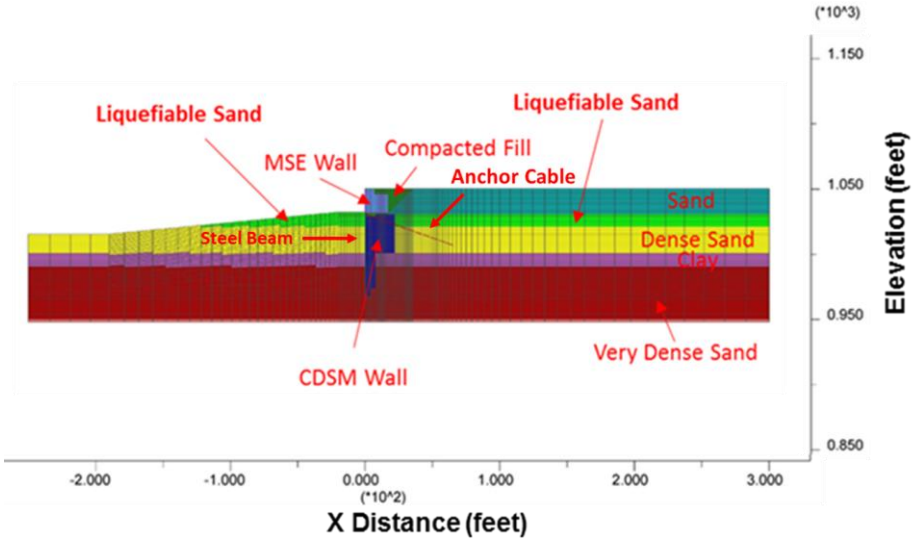


Figure 2. FLAC Model of Base Case Geometry.

### *2.4 Results*

#### *2.4.1 Base Case Geometry*

Figure 3 below presents the summary of results of the modeling of the WRP representative section in terms of lateral displacement along the vertical plane of the MSE and CDSM wall face. The results are shown for three input ground motions and two return periods, 225 years (solid line) and 475 years (dashed line). The lateral displacement profiles suggest two displacements modes: 1) an overall rotation of the CDSM wall; and 2) a sliding of top zone along a plane developed at about 18 feet depth. The sliding plane at 18 feet depth coincides with the top of the soil layer identified as potentially liquefiable, and the interface between the MSE and the CDSM walls. This response is in line with the idealized model of the non-liquefied crust sliding laterally on top of an underlying liquefiable layer towards the free face.

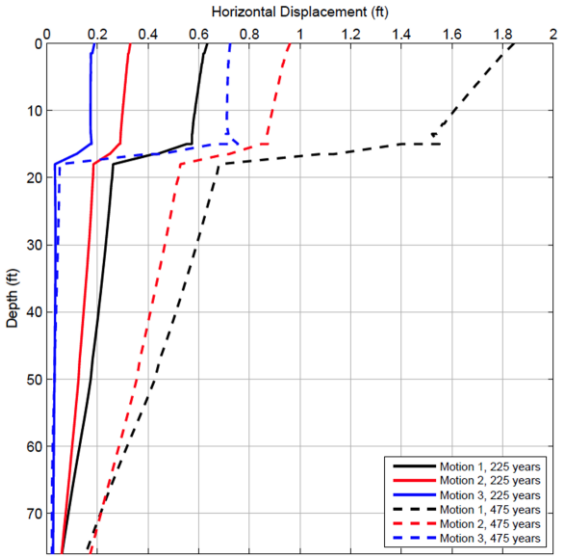


Figure 3. Horizontal Wall Displacements along the MSE and CDSM Wall Face for Base Case

Results for input motion 1 for 475-year return period, which is the motion resulting in the highest seismic lateral displacements shown in Figure 3, is used in further discussion of results and sensitivity runs comparisons. Figure 4 presents the cross-section with horizontal displacement contours for a return period of 475 years and input motion 1. This figure further illustrates the sliding block displacement model that was observed in Figure 3. Figure 4 shows that significant displacement (above 12 inches) were calculated as far as 100 feet behind the MSE wall face. It should be noted that the model assumed horizontally layered soil and did not account for possible non-continuity of the liquefiable soils or liquefaction triggering. Also, with the motion propagated from bottom up, all horizontal layers will be excited in phase, which may not be the case during an actual earthquake.

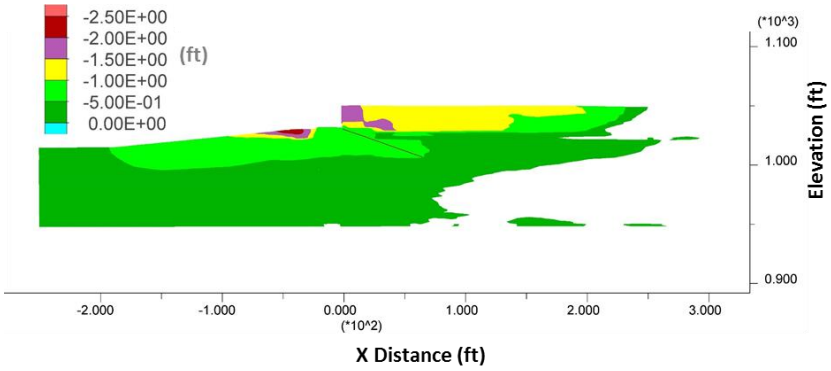


Figure 4. Horizontal Displacement Contours for Base Case (Motion 1, 475-year return period)

*2.4.2 Additional Analysis 1 – Mitigation Alternative*

The results of the base case geometry showed significant wall displacements occurring due to the lateral displacement of the liquefiable soil and crust behind the MSE wall. Hence, additional analysis was conducted by creating a buffer between the weak sliding plane of liquefiable soils and the base of the MSE wall by introducing a zone of improved (or replaced) soil that would not be susceptible to liquefaction. This zone was 5 feet deep (between El. 1030 feet and 1025 feet), and extended 30 feet behind the back of the CDSM wall. The results of this analysis, compared with the base case, are shown below in Figure 5. Inclusion of the non-liquefiable buffer zone decreases the lateral displacements by about one foot (approximately 50 percent), with displacement mode of sliding along the weak plane almost fully eliminated. The buffer zone was included in the final wall design to mitigate liquefaction effects. Figure 6 presents the horizontal displacement contours for this analysis. For this case, surface horizontal displacements are less than 0.5 feet beyond 30 feet from the MSE wall face.

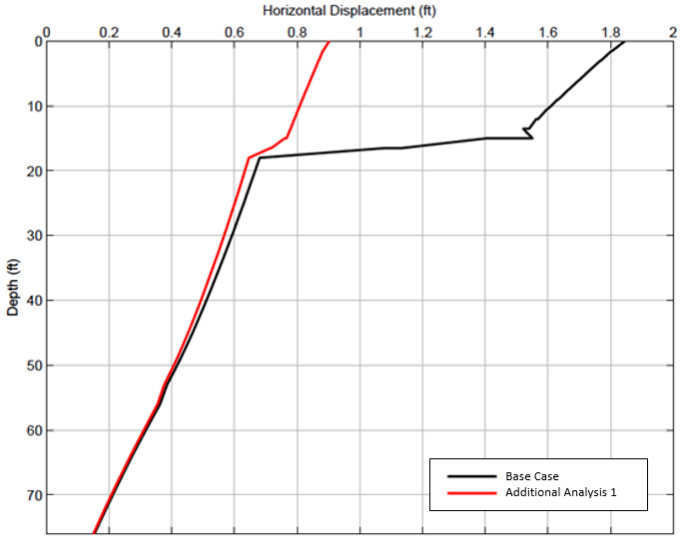


Figure 5. Horizontal Wall Displacements along the MSE Wall Face for Base Case Geometry and Additional Analysis 1

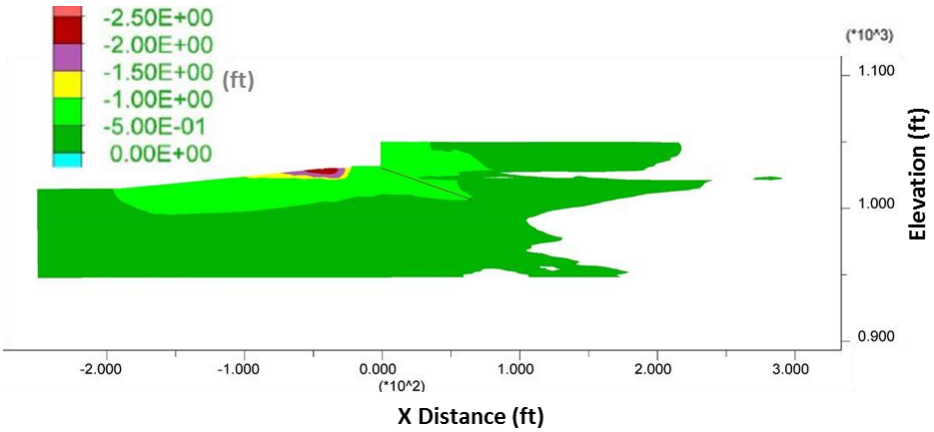


Figure 6. Horizontal Displacement Contours for Additional Analysis 1

*2.4.3 Additional Analysis 2 – Effect of Design Scour Event*

The CDSM wall at the WRP segment is designed to stop the propagation of river scour into the WRP. The significant depth of CDSM wall is required because it was estimated that the scour from the capital flood event could permanently remove significant amount of soil in front of the CDSM wall. In addition, it was estimated that the scour event would temporary suspend up to additional 20 feet of soil and then redeposit it in a looser, potentially liquefiable state. To assess how the wall would perform in case the seismic event occurs following the scour event, three analyses were performed with varying assumptions described below. In addition, different assumptions were made on the groundwater level and liquefaction potential both in front and behind the wall, to assess the results with respect to combination of different critical factors acting combined, i.e., scour and liquefaction. The following combinations were analyzed:

a) Scour of material in front of the CDSM wall (river side) down to El. 1020 feet and loosening of the material down to El. 1000 feet, making it liquefiable – This is the extreme level of possible scour impact. The material behind the wall is consistent with base case. Groundwater level at El. 1030 feet.
b) Scour of material in front of the CDSM wall down to El. 1020 feet without additional loosening of the material between El. 1020 and 1000 feet – This is a less extreme level of possible scour

impact. The material behind the wall is consistent with base case, however, no pore-pressure generation and consequent liquefaction is allowed.

c) Scour of material in front of the CDSM wall down to El. 1020 feet and loosening of the material down to El. 1000 feet, making it liquefiable – This is the extreme level of possible scour impact. The material behind the wall is consistent with base case. Groundwater level at El. 1027 feet This case assumed that highest groundwater level would not coincide with higher shaking.

The results of different cases described above are shown below in Figure 7. This figure shows the impact of liquefaction in front of the wall on the additional wall rotation (red versus green line in the figure), and the impact of water depth on shallow type failure of pushing the MSE wall out (green versus the blue line in the figure). The horizontal displacement at the top of the MSE wall, for scour case a, increased about 20 percent in comparison to the base case showing the significant effect of scour in lateral wall displacements. Additionally, horizontal displacements at the top of the MSE wall were reduced by 45 percent for case b), and by 20 percent for case c), in comparison to case a), illustrating the effect of liquefaction and groundwater table elevation, respectively. Figure 8 illustrates the horizontal displacement contours for the three scour cases. To prevent such high seismic wall displacements, a scour inspection and repair program that included building a buttress in front of the wall in case of significant scour from capital flood, was introduced.

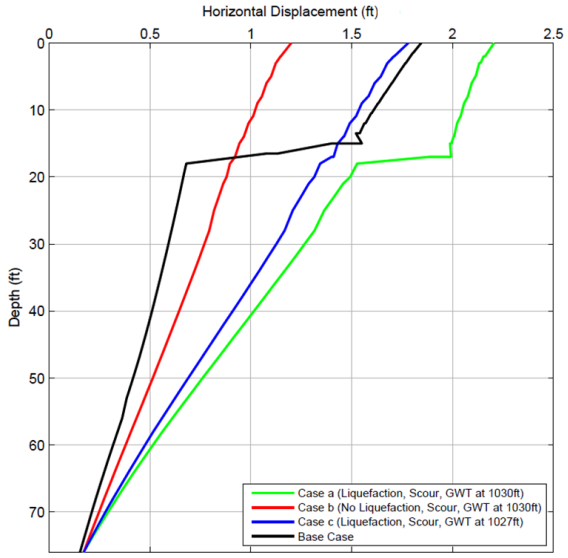


Figure 7. Horizontal Wall Displacements for Additional Analyses 2 (Effect of Scour)

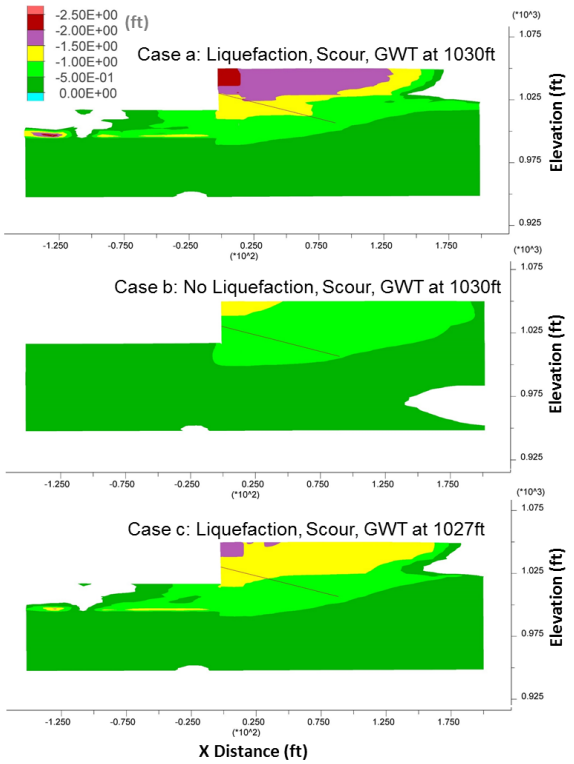


Figure 8. Lateral Displacement Contours for Additional Analyses Including Scour

*2.4.4 Seismic Earth Pressures behind CDSM Wall*

The horizontal earth pressures at the back of the CDSM wall obtained from the base case numerical analysis (Figure 2), have been compared with the pressures estimated based on commonly used simplified relationships, and are presented in Figure 9. The static total horizontal stresses from FLAC are presented in Figure 9 with the blue solid line. The maximum seismic earth pressures from the base case FLAC analysis, for input motion 1 and 475 years return period hazard level, are also plotted with a solid red line.

The simplified static horizontal earth pressures at the back of the CDSM wall were based on Coulomb (1776) and are plotted in Figure 9 with a blue dashed line. The static earth pressures obtained from the FLAC analyses are higher than the pressures based on Coulomb (1776) down to the El. of 1000 feet, while below this elevation, the pressure profiles are in general agreement. The stress concentration behind the CDSM wall at the FLAC model is expected because of the installation of pre-tensioned soil anchors, that increase the horizontal static stresses.

The simplified seismic earth pressures were estimated based on Okabe (1926) and Mononobe and Matsuo (1929), known as the Mononobe-Okabe (M-O) method. M-O method is commonly applied for yielding walls. This method was developed for dry soils. However, since the groundwater table is high at the site, we used the saturated soil unit weight to calculate the total active thrust. The horizontal seismic coefficient ($k_h$) in the M-O method was taken as 100% of PGA, which is 0.62 g for a return period of 475-years. In order to consider the effects of liquefaction at the back of the CDSM wall, the liquefied soil (El. 1030 feet to 1020 feet) was considered as a dense fluid having a unit weight of the liquefied soil (NEHRP 2009). The unsaturated soil above the liquefied soil, was treated as a surcharge that increased the fluid pressure within the underlying liquefied soil (dashed red line in Figure 9). Next, the seismic earth pressure resultant based on the M-O method was distributed as a uniform load along the height of the MSE and CDSM wall. This assumption is conservative since the MSE wall is not rigidly connected to the CDSM wall, allowing sliding of the MSE on the CDSM. This uniform

earthquake load was added to the static earth pressures based on Coulomb (1776), to estimate the total earth pressures behind the CDSM wall along the non-liquefiable soil below the liquefiable layer (El. 1020 to 968 feet) (dashed red line in Figure 9). The seismic earth pressures were also estimated based on Wood (1973) methodology that is applicable for non-yielding walls. The total static and seismic earth pressures based on Wood (1973) (dashed black line) are on the conservative side as presented in Figure 9.

The numerical analyses maximum seismic lateral earth pressures are generally lower (up to about 30 percent lower) than the simplified seismic lateral earth pressures below the El. of 1010 feet. These differences are attributed to the complex geometry of the CDSM wall below El. 1010 feet, the fact that the CDSM wall is buried, and the flexible connection of the MSE and CDSM wall. Above the El. of 1010 feet, the FLAC-based lateral earth pressures behind the CDSM wall are bounded by the simplified earth pressure estimates corresponding to yielding and non-yielding walls. The increased FLAC-based seismic lateral earth pressures are due to the presence of liquefiable soils at the El. of 1030 feet to 1020 feet and as well as due to the pre-tensioned anchors stress concentration.

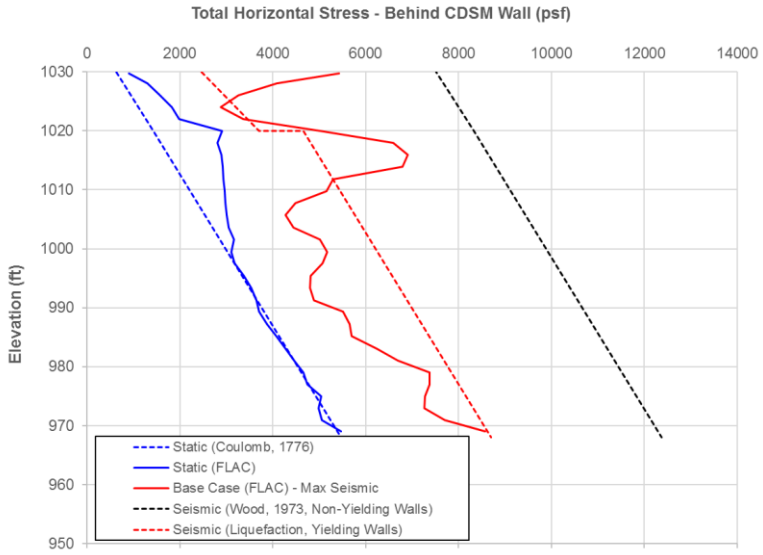


Figure 9. Horizontal Earth Pressures Behind CDSM Wall, Numerical Analyses vs Correlations

## 3. CONCLUSIONS

The effects of liquefaction and scour in the seismic performance of a retaining wall system for a water reclamation plant, located next to a river in a seismically active area, were assessed through advanced numerical analyses using FLAC. Simplified approaches, used in earlier design stages, could not reliably estimate the lateral seismic wall displacements due to the complexity of the anchored retaining wall system and the subsurface conditions. The retaining wall system consisted of an MSE wall, sitting on top of a CDSM wall, tied back with pre-tensioned soil anchors. The advanced numerical analyses were used to develop mitigation approaches for the retaining wall system. The estimated top MSE wall lateral displacements were reduced by approximately 50 percent by creating a buffer between the weak sliding plane of liquefiable soils and the base of the MSE wall. The buffer consisted of a zone of improved (or replaced) soil that would be non-susceptible to liquefaction and was used in the final design to mitigate liquefaction effects. In the event of scour from the capital flood event, lateral seismic wall displacements were estimated to increase about 20 percent in comparison to the base case. Consequently, a scour inspection and repair program was introduced to prevent such high lateral seismic displacements. In addition, the effects of pore pressure generation and consequent liquefaction as well as the effect of groundwater elevation, were investigated through sensitivity

analyses.

Maximum seismic lateral earth pressures from numerical analyses were less conservative than the simplified seismic lateral earth pressures below a certain elevation due to the complex geometry of the CDSM wall, the fact that the CDSM wall is buried, and the non-rigid connection of the MSE and CDSM wall. Above a certain elevation, the FLAC-based seismic lateral earth pressures were bounded by simplified earth pressure estimates corresponding to yielding and non-yielding walls. The increased FLAC-based seismic earth pressures are attributed to the pre-tensioned anchors stress concentration and the presence of liquefiable soils. The FLAC-based horizontal earth pressures allowed for a more realistic CDSM wall design resulting in significant cost savings.

## 4. REFERENCES


Beaty M, Byrne PM, (1998). "An Effective Stress Model for Predicting Liquefaction Behavior of Sand," Proceedings of a Specialty Conference, Geotech. Earthq. Eng. and Soil Dynamics, ASCE pp. 766-777, Seattle.

Coulomb CA (1776). "Essai sur une application des regles des maximis et minimis a quelques problemes de statique relatifs a l'architecture," Memoires de l'Academie Royale pres Divers Savants, Vol. 7.

Mononobe N, Matsuo H (1929). "On the determination of earth pressures during earthquakes," Proceedings, World Engineering Congress, 9p.

NEHRP (2009). "2009 NEHRP Recommended Seismic Provisions for New Buildings and Other Structures," Part 3, Resource Papers (RP) on Special Topics in Seismic Design, RP 12 "Evaluation of Geologic Hazards and Determination of Seismic Lateral Earth Pressures"

Okabe S (1926). "General theory of earth pressures," Journal of the Japan Society of Civil Eng., Vol. 12, No. 1

Giannakou A, Travasarou T, Ugalde J, Chacko MJ, Byrne P, (2011). "Calibration Methodology for Liquefaction Problems Considering Level and Sloping Ground Conditions," 5ICEGE, Chile, paper CMFGI.

Giannakou A, Travasarou T, Chacko MJ (2012). "Numerical Modeling of Liquefaction-Induced Slope Movements," GeoCongress 2012, Oakland, California, March.

ITASCA (2015), "FLAC User's Manual."

Travasarou T, Chen W, Chacko MJ (2011). "Liquefaction-Induced Uplift of Buried Structures – Insights from the Study of an Immersed Railway Tunnel," 5ICEGE, Chile, paper LITUR.

Travasarou T, Chacko MJ, Chen WY, Giannakou A, Ilankatharan M, Ugalde J (2012). "Application of Advanced Numerical Methods to assess Seismic Performance for Major Projects," Proceedings, 2nd International Conf. on Performance Based Design in Earthquake Geotechnical Engineering, Taormina, Italy, May, Paper 7.11.

Wood J (1973). "Earthquake-induced soil pressures on structures," Report EERL 73-05, California Institute of Technology, Pasadena, California, 311 pp.